NOTES AND CORRESPONDENCE

The Motion of a Solid Sphere in an Oscillating Flow: An Evaluation of Remotely Sensed Doppler Velocity Estimates in the Sea

DAVID A. SIEGEL

Department of Geography, University of California at Santa Barbara, Santa Barbara, California

ALBERT J. PLUEDDEMANN

Woods Hole Oceanographic Institution, Woods Hole, Massachusetts

4 April 1990 and 23 October 1990

ABSTRACT

Several popular techniques employed to remotely sense oceanic velocity fields utilize the Doppler shifts of backscattered radiation (such as sound or light) from suspended particles to estimate fluid velocities. Implicit in this use is the assumption that the motion of the particles and the fluid parcels about them is identical. Here, a simple dynamical model of a solid sphere in a unidirectional oscillating flow is used to evaluate the effects of differential particle motion on remotely sensed Doppler velocity estimates. The analysis indicates that typical oceanic particles will move with the fluid if their density is equal to the fluid's density or if the oscillation frequency (ω) is less than a critical frequency ($\omega_c = 0.1\nu a^{-2}$; where ν is the kinematic viscosity of the fluid and a is the particle radius). For oscillation frequencies greater than ω_c, the particle and flow velocities diverge significantly from each other. Particle motion will be amplified for particles less dense than the fluid and reduced for relatively heavy particles. The motions of particles and the fluid may have significant phase differences as well. Critical frequencies are estimated for some common oceanic particles enabling the performance of several Doppler velocity measurement techniques to be evaluated. The present results indicate that for some oceanographic applications the Doppler sensing of fluid velocities using particulate backscatter may be limited by the inability of the particles to follow the fluid motion. The model results suggest that it is possible to correct for the velocity differences between the particle and its fluid parcel if the size and relative density of the backscattering material is known. This strongly indicates that a greater emphasis must be placed on the characterization of the materials that are producing the backscattered signals.

1. Introduction

Remote sensing techniques that use the Doppler shifts from backscattered radiation signals to sample the oceanic velocity field have become increasingly popular in recent years. Many ships are now equipped with acoustic Doppler profilers to make velocity measurements while underway, and self-contained Doppler instruments suitable for deployment on the ocean bottom or from moorings have been developed. Doppler remote sensing techniques have proven useful in obtaining the velocity field for mesoscale motions (e.g., Regier 1982), fronts (e.g., Trump et al. 1985), internal waves (Pinkel 1981, 1983; Chereskin et al. 1989), near-surface mixed layer motions (Smith et al. 1987), surface gravity waves (Pinkel and Smith 1987; Krogstad et al. 1988), and even turbulent motions (e.g., Veth 1980; Lhermitte and Poor 1983; Agrawal and Belting 1988).

Corresponding author address: Dr. David A. Siegel, Dept. of Geography, 3611 Ellison Hall, University of California at Santa Barbara, Santa Barbara, CA 93106.

Implicit in the interpretation of the Doppler data is the assumption that the material that produces the backscattered signal is advected exactly with the fluid. In one's personal experiences, many examples where the motion of particles are different from the flow around them can be recognized; such as snowflakes falling in a breeze, leaves blowing across a field, pieces of twigs in a stream, or bubbles in a glass of beer. A portion of this differential motion, especially in the vertical, is caused by Stokes settling, where the viscous drag and the buoyancy forces on the particle are balanced (e.g., Clift et al. 1978). However, the fact that there is a Stokes settling velocity implies that the particles have an inertia different from the fluid parcel about them. As will be shown, this difference in inertia between the particle and its fluid parcel can lead to differential motions for particular time scales.

In the following, a simple model of the motion of a solid sphere in an oscillating flow is developed and employed to evaluate the correspondence between particle and fluid motions. A schematic diagram for this model, illustrating the parameters used in this problem, is shown in Fig. 1. The procedure to be employed is to

examine the frequency response of a sphere forced by an oscillating flow. Deviations from unitary response will show up in both the amplitude and the phase of the frequency response function for frequencies above a particular critical value. For common oceanic particulates, values of this critical frequency are evaluated and possible limitations of oceanic Doppler velocity remote sensing are discussed.

2. Motion of a solid sphere in an oscillating flow

The model is developed using the equations of motion for a solid sphere in a nonuniform flow formulated by Maxey and Riley (1983) (hereafter, MR83). The force balance for a spherical particle in an unsteady, nonuniform flow is given as

$$\underset{\text{A}}{m_p \frac{dV_i}{dt}} = \underset{\text{B}}{(m_p - m_f)g_i} + \underset{\text{C}}{m_f \frac{Du_i}{Dt}} - \underset{\text{D}}{\frac{m_f}{2}\frac{d}{dt}\left(V_i - u_i - \frac{a^2}{10}\nabla^2 u_i\right)} - \underset{\text{E}}{6\pi\rho_f a\nu(V_i - u_i)} + \underset{\text{F}}{\frac{3}{4} m_f \nu \nabla^2 u_i} - \underset{\text{G}}{6\rho_f a^2(\pi\nu)^{1/2}\int_0^t \frac{\frac{d}{dz}\left(V_i - u_i - \frac{a^2}{6}\nabla^2 u_i\right)}{(t-\tau)^{1/2}}\, d\tau} \quad (1)$$

where V_i is the velocity of the particle in the ith direction, u_i is the fluid velocity at the center of the particle $[Y(t)]$, a is the particle's radius, m_p is the mass of the particle ($m_p = \frac{4}{3}\rho_p \pi a^3$), m_f is the mass of a fluid sphere with radius a ($m_f = \frac{4}{3}\rho_f \pi a^3$), ρ_p is the particle density, ρ_f is the fluid density, ν is the kinematic viscosity of the fluid, and g_i is the acceleration due to gravity. The Laplacian operator (∇^2) is evaluated at the center of the sphere $[Y(t)]$, the convective derivative $D(\ )/Dt$ equals $[\partial(\ )/\partial t + u_i \partial(\ )/\partial x_i]_{Y(t)}$, and the convective derivative $d(\ )/dt$ is equal to $[\partial(\ )/\partial t + V_i \partial(\ )/\partial x_i]_{Y(t)}$.

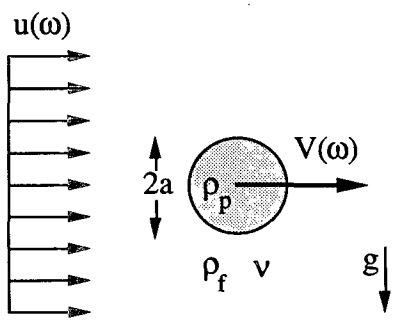

FIG. 1. Schematic diagram of the model problem to be discussed. The solid sphere has a radius equal to a and its density is equal to ρ_p. The fluid density (ρ_f) is assumed to be 1025 kg m^{-3} and the molecular viscosity (ν) is taken to be 10^{-6} m^2 s^{-1}. The oscillating, spatially uniform flow of the fluid, $u(\omega)$, drives the particle's motion, $V(\omega)$. The acceleration due to gravity (g_i) acts downward.

The MR83 equation is valid for the motion of solid spheres for a temporally and spatially varying flow under the conditions that (i) the Reynolds number based upon the sphere radius and the velocity difference between the free-stream and particle is much less than one (that is, $\mathrm{Re}_{\mathrm{rel}} = a|V_i - u_i|\nu \ll 1$) and (ii) that the particle radius, a, is smaller than the smallest scale in the flow, l. However, the velocity field is allowed to vary slowly over the spatial extent of the particle (i.e., $l > a$). In addition, the MR83 formulation assumes that the sphere's motion cannot affect the flow field, the particles cannot interact with each other, and modifications to the calculated drag caused by particle rotation must be negligible.

The MR83 expression [Eq. (1)] states that the acceleration of the particle (term A) is controlled by the relative buoyancy of the particle (B), the fluid acceleration acting on the particle (C), the force required to move water around the particle [the added mass force (D)], the viscous Stokes drag on the sphere (E), the Faxen correction for the Stokes drag due to nonuniform flows (F), and the Basset term (G), which is a correction to the Stokes term for time variations in the drag force. The Laplacian operators in the added mass (D) and Basset term (G) are additional Faxen corrections for the drag caused by nonuniformity in the fluid velocity field. The derivation and detailed interpretation of the equation of motion for a solid sphere in a nonuniform flow field may be found in MR83.

For steady particle motion in a quiescent fluid ($u_i = 0$), the MR83 equation of motion reduces to a balance between the buoyancy and Stokes drag forces [terms B and E in Eq. (1)]. The resulting velocity, the Stokes settling velocity (V_{si}), is equal to

$$V_{si} = \frac{2(\gamma - 1)a^2 g_i}{9\nu} \quad (2)$$

where γ is the density of the particle relative to the fluid ($=\rho_p/\rho_f$). Thus, relatively heavy particles ($\gamma > 1$) will have a Stokes velocity in the direction of the gravitational acceleration, while lighter particles will have an opposite Stokes settling velocity. The definition of the Stokes settling velocity enables the instantaneous particle velocity (v_i) to be partitioned into a steady portion (V_{si}) and a residual perturbation velocity ($v_i - V_{si}$).

For a spatially uniform flow, as in the model problem (Fig. 1), the spatial derivative terms in the MR83 equation [Eq. (1)] are identically zero. The resulting equation, when written in nondimensional form, may be expressed as

$$(2\gamma + 1)\frac{dv_i}{dt} = 3\frac{du_i}{dt} - 9(v_i - u_i) - \frac{9}{(\pi)^{1/2}}\int_0^t \frac{(dv_i/d\tau - du_i/d\tau)}{(t-\tau)^{1/2}}\,d\tau \quad (3)$$

where v_i now denotes the perturbation particle velocity ($v_i - V_{si}$), and time has been nondimensionalized using the viscous time ($\tau_\nu = a^2/\nu$). This relation is referred to as the Basset–Boussinesq–Oseen (BBO) equation and holds for the motion of a small solid sphere in a spatially uniform, but temporally varying, flow (e.g., Clift et al. 1978). The BBO equation may be also derived from the MR83 equation under the limit that the smallest scale in the flow, l, is much larger than the particle's radius ($l \gg a$). That is, the BBO equation will hold for a spatially nonuniform flow under the condition that the velocity field does not vary over the scale of the particle.

As the BBO equation is linear, the particle velocity may be solved for in terms of the fluid velocity using Fourier series expansions,

$$v_i = \int_{-\infty}^{\infty} \hat{v}_i \exp(i2\pi\omega t)\,d\omega$$

$$u_i = \int_{-\infty}^{\infty} \hat{u}_i \exp(i2\pi\omega t)\,d\omega \quad (4)$$

where ω is the cyclic nondimensional frequency, $i = \sqrt{-1}$, and $\hat{v}_i$ and $\hat{u}_i$ are the Fourier coefficients for the particle and fluid velocities, respectively. Applying the Fourier series expansions to the BBO equation, the Fourier coefficients for the particle and fluid velocities are related by,

$$\hat{v}_i = H(\omega; \gamma)\hat{u}_i \quad (5a)$$

where

$$H(\omega; \gamma) = \frac{6\pi\omega i + 9 + 9(\pi\omega)^{1/2}(1-i)}{(2\gamma+1)2\pi\omega i + 9 + 9(\pi\omega)^{1/2}(1-i)} \quad (5b)$$

is the frequency response function relating the particle velocity to the fluid velocity and is a function of the nondimensional frequency, ω, and the reduced density, γ. The magnitude and phase of $H(\omega; \gamma)$ are shown in Fig. 2a for values of γ ranging from 0 to 5 and in Fig. 2b for values of γ ranging from 0.8 to 1.2. This expression [Eq. (5)] is similar to that derived by Hjelmfelt and Mockros (1966).

If the reduced density, γ, is equal to one, the response function, $H(\omega; \gamma)$, is equal to unity for all nondimensional frequencies [Eq. (5)]. Thus, a solid sphere with a density equal to the fluid's density will move exactly with the spatially uniform flow. However if γ deviates from unity, differential motion can occur for some frequencies (Fig. 2).

For low nondimensional frequencies ($\omega < 0.1$), there is little difference between the particle and the fluid motions, and a unit frequency response is observed. This can be seen in the asymptotic values of the frequency response function for very low frequencies [$H(\omega \to 0; \gamma) = 1$, for all γ]. At these low frequencies, the viscous drag force dominates the dynamics of the sphere's motion [term E in Eq. (1)]. In a sense, the water is so viscous that the sphere "sticks" to the fluid parcel mimicking its motion exactly. Thus, one would expect unit frequency response in amplitude and zero phase differences.

For reduced particle densities, γ, less than about 3, a nondimensional frequency of 0.1 appears to act as a critical value separating frequencies where differential motion is apparent from frequencies of unit response (Fig. 2). We will denote a nondimensional frequency of 0.1 as this critical frequency. In dimensional terms, the critical frequency (ω_c) is equal to

$$\omega_c = \frac{0.1\nu}{a^2}. \quad (6)$$

Thus, in a fluid with fixed kinematic viscosity like the ocean, differential motions can occur because of high oscillation frequencies, large particle sizes, or both.

Relatively light particles ($\gamma < 1$) tend to exaggerate and lead the fluid oscillations; while relatively dense particles respond in the opposite fashion (Fig. 2). The amplification of particle motion is especially apparent for the higher nondimensional frequencies where asymptotic values are observed [$H(\omega \to \infty; \gamma) = 3/(2\gamma + 1)$]. For relatively light particles, the asymptotic value of $H(\omega \to \infty; \gamma)$ is equal to 3; while for heavy particles it is equal to $3/(2\gamma)$. At these high frequencies, the acceleration of the particle [term A in Eq. (1)] is balanced by the force applied to the particle by the fluid (C) and the force required to move water out of the path of the particle (D; the added mass term without the Laplacian term). The asymptotic values for the amplitude of the response function arise because of the difference between the mass of the particle and the mass of a fluid sphere of equal volume. It should also be noted that there are no phase differences between the motion of the particle and the fluid at these high frequencies (Fig. 2).

Significant phase differences are found predominantly for nondimensional frequencies between 0.1 and 10 (Fig. 2). The phase differences are generally small for values of γ close to one (usually less than 10°; Fig. 2b), however for values of γ much different than one, the phase differences may be quite large ($\sim \pm 60°$; for $\gamma = 0$ or 5; Fig. 2a). These phase differences come about largely due to the effects of the Basset "history" term [term G in Eq. (1)].

For very heavy particles ($\gamma > 10$), the critical frequency separating unit particle response from differential motion decreases rapidly with increasing relative particle density. This case is not of present concern as there are very few naturally occurring particles in the

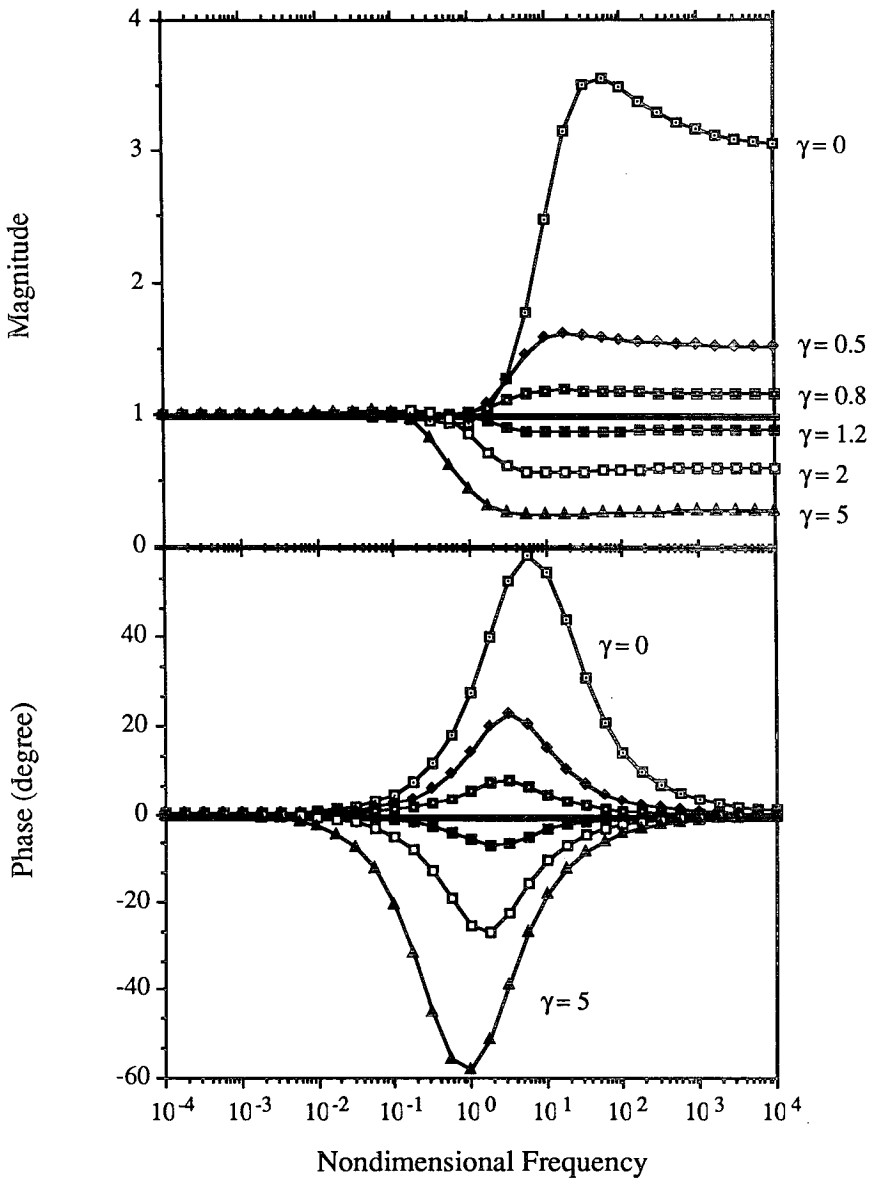

FIG. 2a. Magnitude and phase of the frequency response function $[(H(\omega; \gamma)]$ for γ = 0, 0.5, 0.8, 1, 1.2, 2, and 5. A magnitude greater than one indicates that the particle will overamplify the fluid's oscillation. A positive phase means that the particle is leading the fluid oscillation. Note that high nondimensional frequencies correspond to relatively small particle sizes as well as rapid fluid oscillations.

sea that would have values of γ greater than 10 (for example, a lead sphere in seawater has a γ equal to 11). However, it should be noted that these considerations may be relevant to the application of Doppler velocity estimation to the sampling of atmospheric motions using liquid-water droplets ($\gamma \sim 1000$).

3. Doppler velocity estimation in the sea

It has been shown that differential motion between spherical particles and the fluid about them will take place for cyclical frequencies greater than some critical value ($\omega_c = 0.1\nu a^{-2}$). Differences in magnitude are persistent in the sense that at frequencies greater than ω_c they asymptote to values that are a function of the reduced density of the particle alone (Fig. 2). In this same sense, the differences in phase are transient, with deviations between the phases of oscillation occurring for values of nondimensional frequency roughly between 0.1 and 10 (dimensional frequencies between $0.1\nu a^{-2}$ and $10\nu a^{-2}$).

Persistent amplification or reduction of relative particle motion has obvious implications for remotely

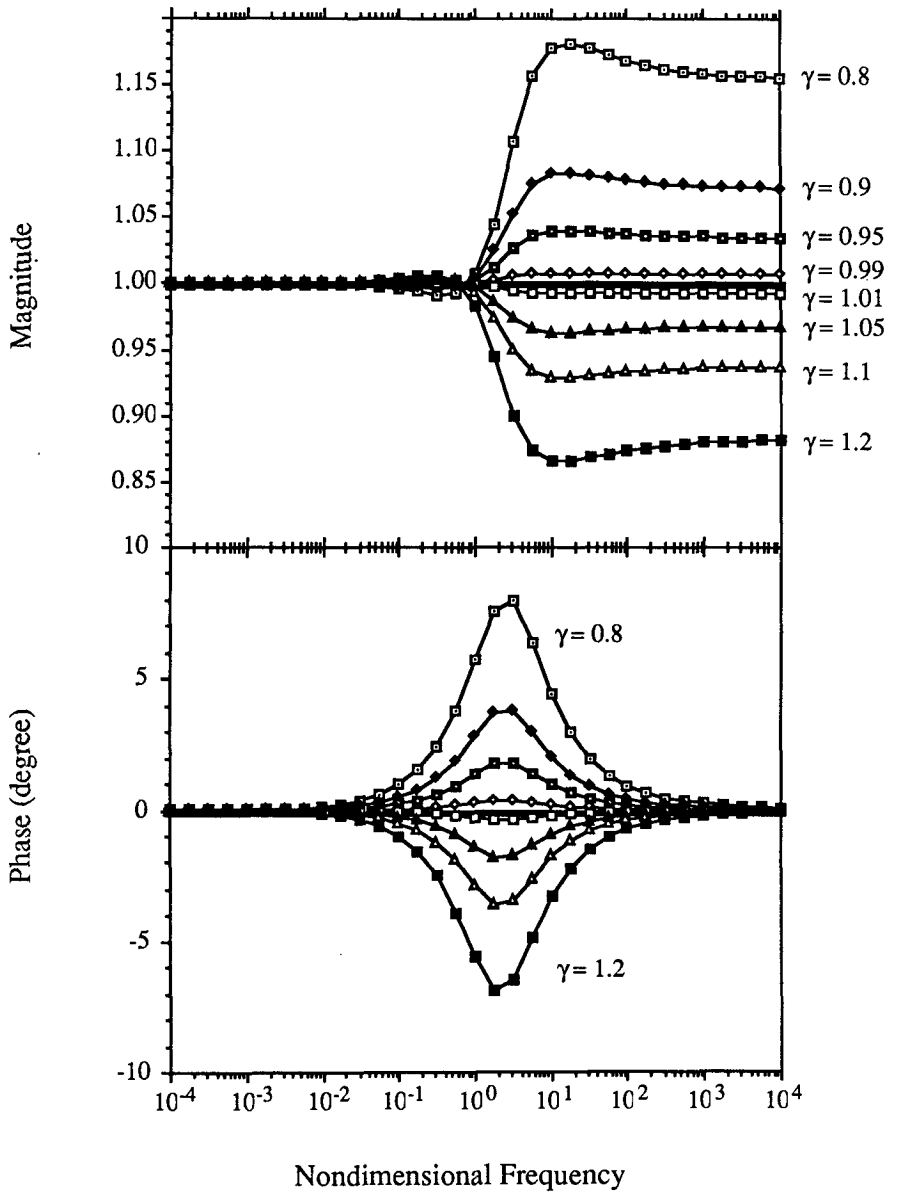

FIG. 2b. Magnitude and phase of the frequency response function $[H(\omega; \gamma)]$ for γ = 0.8, 0.9, 0.95, 0.99, 1 (the thick solid line), 1.01, 1.05, 1.1, and 1.2.

sensed Doppler velocity determinations. Clearly, the magnitude of oscillatory flows will be improperly estimated for frequencies greater than ω_c. This source of estimation error may lead to biases in mean flow determinations, particularly if the sampling of the higher frequency motions is aliased. For frequencies where large phase deviations are found, difficulties may arise in comparing the Doppler velocity estimates to coincident scalar measurements such as temperature, salinity, or acoustic backscatter intensity.

In evaluating the effects of differential particle motions on oceanographic Doppler velocity estimation, one must consider both the characteristics of the backscattering particles and the flow in which they are advected. At issue is the possibility that some oceanographic Doppler velocity measurements may be "fluid mechanically limited" by the inability of the observed particles to track the fluid's motion. The basis of our evaluation of Doppler velocity estimation is the characterization of the critical frequencies for typical oceanic particles. A tabulation of characteristic sizes and relative densities for some common backscattering particles and their corresponding critical frequencies is presented in Table 1. A discussion of some of the more important particle–seawater systems is presented in the following section.

a. Zooplankton as backscattering targets

At present, the most widespread use of acoustic Doppler techniques in the sea involves the deployment of multibeam, range-gated current profiling devices. Measurements made within the ocean interior, outside of the near-surface or bottom boundary layers, rely primarily on backscattered signals from macrozooplanktonic organisms. Typical acoustic profilers operate at frequencies between 50 kHz and 1 MHz. At these frequencies the targets are likely to be organisms such as pteropods (Hansen and Dunbar 1971), decapods (Pearcy and Mesecar 1971), copepods (Castile 1975), and euphausiids (Pieper 1979). The equivalent spherical radii (the radius of a sphere equal in volume to the displaced volume of the particle) for these organisms range from roughly 50 to 4000 μm and the resulting critical frequencies are between 40 cycles per second (c s^{-1}) and 22 c h^{-1} (Table 1).

The most common acoustic velocity profilers use the pulse-to-pulse incoherent processing technique (e.g., Pinkel 1981; 1983), which is best suited to the measurement of motions with characteristic spatial scales of several meters or more. Incoherent Doppler systems achieve high velocity precision [O(1 cm s^{-1})] only after averaging together the returns from many consecutive acoustic pulses. Thus, this technique is typically employed for the observation of motions with frequencies of a few cycles per hour or less. Velocity estimation using incoherent systems are generally well matched to the limits imposed by differential motion of the scatterers since most observed flows (currents, eddies, tidal and inertial oscillations, internal waves, etc.) have characteristic frequencies much less than the lower critical frequency.

Recently, pulse-to-pulse coherent acoustic Doppler systems have been used to measure small-scale (<10 m) velocity fields. Coherent Doppler systems can achieve 1 cm s^{-1} velocity precision for fluid oscillation frequencies as high as 1 c s^{-1} and thus may be used for the observation of high-frequency internal waves (Sherman 1989) and turbulence (Lhermitte and Poor 1983). If the acoustic scatterers have equivalent spherical radii larger than 300 μm then the critical frequency will be 1 c s^{-1} or less, well within the frequency range of the motions that the instruments are attempting to measure. For this case, measurement errors are expected due to differential motion between the fluid and the scatterers. However, typical densities for zooplanktonic organisms are near that for seawater, which indicates that these errors should be small. For a scatterer with a reduced density of $\sim$1.04 (Greenlaw and Johnson 1982), the maximum magnitude error will be about 3% and the maximum phase error will be less than 2° (Fig. 2b).

TABLE 1. Critical frequencies for some particle–seawater systems.

Particle	Application	a (μm)	γ	ω_c
Zooplankton[a]	Sonar	50–4000	1.04	40 c s^{-1}–22 c h^{-1}
Beach sand[b]	Sonar/laser	30–500	2.6	111 c s^{-1}–24 c m^{-1}
Bubbles[c]	Sonar/laser	20–300	0.00115	250 c s^{-1}–1.1 c s^{-1}
BBL sediments[d]	Sonar/laser	0.1–60	1.4–2.6	10^7–28 c s^{-1}
Phytoplankton[e]	Laser	1–100	1.0–1.3	10^5–10 c s^{-1}
Bacteria[e]	Laser	0.1–1	1.03–1.2	10^7–10^5 c s^{-1}

[a] The majority of zooplankton biomass lies in the size range between 50 and 2000 μm radius (e.g., Sheldon et al. 1972; Costello et al. 1989). Combined acoustic and biological sampling indicates that in the frequency range commonly used by acoustic Doppler instruments (50 kHz to 1 MHz) the principal scatterers are larger zooplankton with equivalent spherical radii of up to 4000 μm (Pieper 1979; Greenblatt 1981; Stanton et al. 1987; Flagg and Smith 1989). The value of γ is from Greenlaw and Johnson (1982).

[b] Beach sand is principally quartz, which has a density of 2650 kg m^{-3} and ranges in size from 62 to 1000 μm in diameter according to the Wentworth scale (Inman 1963).

[c] Significant bubble populations are found with radial dimensions ranging from 20 to 300 μm, with a peak in the populations near 50 μm (Wu 1988).

[d] Suspended sediments within the benthic boundary layer (BBL) are often composed of silt, clay, or various aggregates that may contain high fractions of organic materials. Clay and silt particles range from 0.24 to 62 μm diameter on the Wentworth scale (Inman 1963) and have a density similar to quartz (2650 kg m^{-3}). Organic aggregates have been observed with typical sizes of about 10 μm and densities of about 1400 kg m^{-3} (Pierce 1976). Observations above the Nova Scotian Rise indicate that small particles (2–8 μm) were comprised primarily of mineral while larger particles (20–60 μm) were comprised of mucus-dominated organic aggregates with values of γ of $\sim$1.12 (McCave 1985).

[e] Bacteria and phytoplankton have radii ranging from 0.1 to 1 μm and 1 to 100 μm, respectively (e.g., Parsons et al. 1984). Densities for these particles are similar to seawater with values of γ ranging from 1.03 to 1.19 for bacteria (Simon and Azam 1989) and from 1.005 to 1.27 for phytoplankton (Mitchell et al. 1989).

b. Bubbles as targets

Recent work has demonstrated that Doppler techniques can be used to measure the orbital velocities of surface gravity waves enabling the horizontal wavenumber–frequency spectrum to be inferred (Pinkel and Smith 1987: Krogstad et al. 1988). The scatterers in this case are thought to be a thin (about 1 m) layer of air bubbles just beneath the air–sea interface (Smith 1989). The solid sphere model described here is not adequate for describing the dynamics of air bubbles (or any other fluid sphere) in an oscillating flow. This is because the viscous drag on a fluid sphere is reduced by the induced internal circulations (Batchelor 1973; Clift et al. 1978). This will also alter the derivation of the MR83 equation of motion [Eq. (1)], so a simple alteration of the viscous drag term [term E in Eq. (1)] will not be valid. However at high nondimensional frequencies, the balance of forces acting on the solid sphere is between the unsteady and added mass terms [terms A, C, and D in Eq. (1)]. None of these terms are directly related to the viscous forces acting on the sphere or the fluid viscosity. Thus, the high-frequency asymptotic limits derived for the solid sphere in an oscillating flow should also hold for the case of the

fluid sphere. Unfortunately, the detailed evaluation of this case is beyond the scope of the present contribution.

Assuming that the results based on the solid sphere model are representative for an air bubble in seawater, we find that the lowest critical frequency is near the energy containing portion of the surface wave spectrum (Table 1). For scattering near the peak of the bubble-size spectrum (50 μm; Wu 1988) the value of ω_c is 40 c s^{-1}, high enough to allow measurement of wind waves and swell with minimal error, but well within the range of frequencies where capillary waves are important (10–150 c s^{-1}; Phillips 1980).

The limitations of acoustic Doppler sensing of fluid velocities using bubbles as the backscattering targets may be reduced by "tuning" the acoustic frequency used. The resonant frequency of an air bubble in seawater at atmospheric pressure (f_r in Hz) is related to the bubble radius by

$$f_r = \frac{3.26 \times 10^6}{a} \tag{7}$$

where the bubble radius (a) is in units of microns (μm) (Urick 1983). Assuming that the backscattered returns are dominated by those bubbles whose resonant frequency matches the acoustic frequency, increasing the acoustic frequency will mean that resonant returns will come from the smaller-sized bubbles of the population. With smaller-sized bubbles as targets, the critical frequency will be increased. This will reduce the likelihood of distorted observations of capillary waves and the high-frequency end of the surface gravity wave spectrum.

c. *Other suspended materials as targets*

Many other types of particles may be used as targets for the Doppler determination of velocity (see Table 1). For measurements of turbulence in the benthic boundary layer or the surf-zone, it appears that the critical frequencies for larger suspended sediments and beach sands may be too low to allow the limitations of differential particle–fluid motions to be ignored. The large values of reduced density for sand and sediments means that the errors due to differential motion will be significant. For a particle with density of quartz ($\gamma = 2.6$), the magnitude of these oscillatory motions may be underestimated by as much as 50% and phase errors can be as large as 35°. However, the Doppler estimate of particle motion will be (by definition) the correct velocity to use for the estimation of suspended material transport. The use of biogenic materials such as phytoplankton or bacteria cells as backscattering targets for laser light does not appear to be fluid mechanically limited since the critical frequencies for all but the largest particles are well above the frequencies of interest for oceanographic flows.

d. *Caveats*

Although the simple theoretical criteria presented here will hold for small solid spheres, its application to arbitrary oceanic particles contains many caveats, some of which will be addressed here. First, very few particles in the sea are solid spheres. Zooplanktonic organisms are often shaped similar to bent cylinders with multiple appendages; while sand particles are often multiply faceted and can be more cubic in shape than spherical. For these particles, the simple model presented will not hold. Any morphological deviation from a perfect sphere will act to induce additional motions, such as rotation, which will cause the particle motion to deviate from its fluid parcel. For example, particle rotation can give rise to lift forces (e.g., Clift et al. 1978), which is not considered by MR83. It is conceivable that irregularly shaped particles will have a greater viscous drag than would a sphere of equal volume. However for frequencies greater than ω_c, the dominant balance of forces does not include the viscous drag force. Thus for these time scales, irregularity in the particle's shape may give rise to accentuated differential motions because of the effects of particle rotation.

Second, it was assumed in deriving the BBO equation that the flow is uniform over the scale of the particle (i.e., $l \gg a$). This assumption may not always be satisfied for all flows and all particle types. The smallest dynamical scale in a fully developed turbulent flow is related to the Kolmogorov length scale, L_k,

$$L_k = \left(\frac{\nu^3}{\epsilon}\right)^{1/4} \tag{8}$$

where ϵ is the turbulent kinetic energy dissipation rate. The Kolmogorov length defines the scale where molecular viscosity and inertial turbulent processes equally influence the dynamics of the flow (e.g., Tennekes and Lumley 1972). Typical oceanic values for L_k range from $\sim$300 μm ($\epsilon = 10^{-4}$ m^2 s^{-3}) to $\sim$5600 μm ($\epsilon = 10^{-9}$ m^2 s^{-3}; Lueck and Reid 1984). From examination of Table 1, it can be seen that many oceanic particles have radii larger than L_k, violating the condition $l \gg a$. If the particle radius is larger than L_k, the particle motion will, in a sense, respond to fluid velocity averaged over the extent of the particle. For this case, the motion of the particle will surely be different than the fluid parcels about it.

Third, many zooplanktonic organisms are motile and can swim at velocities that may be comparable to or greater than the velocity of the surrounding fluid. In particular, these organisms are often observed to execute diurnal vertical migrations with vertical swimming speeds of up to 5 cm s^{-1} (e.g., Parsons et al. 1984). These purely biological motions represent non-fluid velocities that can appear as a strong Doppler signal (Plueddemann and Pinkel 1989) and must be

considered in the interpretation of Doppler velocity estimates where zooplankton are the acoustic targets.

The above caveats all address additional processes that cause the motion of a particle to deviate from its fluid parcel. These processes will act in addition to the simple fluid mechanical theory discussed. In this sense, the simple theory of the motion of a solid sphere in an oscillating, spatially uniform flow will represent a "best-case" evaluation of oceanic Doppler velocity determinations. The caveats described above should act only to exacerbate the situation.

4. What next?

The simple model presented indicates that Doppler velocity estimation techniques may be limited for some oceanographic applications by the inability of some particles to follow the fluid motion. Examples of space and time scales where this fluid mechanical limitation becomes important were given for several typical particle–seawater systems. In principle, these limitations can be "corrected" by inverting the spectral response function [$H(\omega; \gamma)$; Eq. (5)] to determine the Fourier coefficient for the required fluid velocity, $\hat{u}_i$, in terms of the sampled particle velocity spectrum, $\hat{v}_i$, or

$$\hat{u}_i = H(\omega; \gamma)^{-1}\hat{v}_i. \qquad (9)$$

In order to perform this inversion, both the size and relative density of the particulate materials that have produced the Doppler signals must be well known. This strongly indicates that a greater emphasis must be placed on the characterization of the materials that are producing the backscattered signals. This, along with measurements of backscattering signal strength and derived Doppler velocity, may be the only practical method by which oceanic Doppler velocity estimation techniques can be extended to frequencies near and beyond the critical frequency.

Acknowledgments. Our work has been funded by the Office of Naval Research under Grant N00014-89-J-1683. Comments on the manuscript by Roger Samelson, Jim Churchill, Tim Stanton, and the anonymous reviewers are gratefully acknowledged. Woods Hole Oceanographic Institution contribution number 7354.

REFERENCES

Agrawal, Y. C., and C. J. Belting, 1988: Laser velocimetry for benthic sediment transport. *Deep-Sea Res.*, **35,** 1047–1067.

Batchelor, G. K., 1973: *An Introduction to Fluid Dynamics.* Cambridge University Press, 615 pp.

Castile, B. D., 1975: Reverberation from plankton at 330 kHz in the Western Pacific. *J. Acoust. Soc. Amer.*, **58,** 972–976.

Chereskin, T. K., M. D. Levine, A. J. Harding and L. A. Regier, 1989: Observations of near-inertial internal waves in acoustic Doppler current profiler measurements made during the Mixed Layer Dynamics Experiment. *J. Geophys. Res.*, **94,** 8135–8145.

Clift, R., J. R. Grace and M. E. Weber, 1978: *Bubbles, Drops and Particles.* Academic Press, 285 pp.

Costello, J. H., R. E. Pieper and D. V. Holliday, 1989: Comparison of acoustic and pump sampling techniques for the analysis of zooplankton distributions. *J. Plank. Res.*, **11,** 703–709.

Flagg, C. N., and S. L. Smith, 1989: On the use of the acoustic Doppler current profiler to measure zooplankton abundance. *Deep-Sea Res.*, **36,** 455–474.

Greenblatt, P., 1981: Sources of acoustic backscattering at 87.5 kHz. *J. Acoust. Soc. Amer.*, **70,** 134–142.

Greenlaw, C. F., and R. K. Johnson, 1982: Physical and acoustical properties of zooplankton. *J. Acoust. Soc. Amer.*, **72,** 1706–1710.

Hansen, W. J., and M. J. Dunbar, 1971: Biological causes of scattering layers in the Arctic Ocean. *Proc. Inter. Sym. on Biological Sound Scattering in the Ocean.* Report No. MC-005, G. B. Farquhar, Ed., Maury Center for Ocean Science, 508–526,

Hjelmfelt, A. T., Jr., and L. F. Mockros, 1966: Motion of discrete particles in a turbulent fluid. *Appl. Sci. Res.*, **16,** 149–161.

Inman, D. L., 1963: Sediments: Physical properties and mechanics of sedimentation. *Submarine Geology,* F. P. Shepard, Ed., Harper and Row, 101–151.

Krogstad, H. E., R. L. Gordon and M. C. Miller, 1988: High-resolution directional wave spectra from horizontally mounted acoustic Doppler current meters. *J. Atmos. Ocean. Technol.*, **5,** 340–352.

Lhermitte, R., and H. Poor, 1983: Multibeam Doppler sonar observations of tidal flow turbulence. *Geophys. Res. Lett.*, **10,** 717–720.

Lueck, R., and R. Reid, 1984: On the production and dissipation of mechanical energy in the ocean. *J. Geophys. Res.*, **89,** 3439–3445.

McCave, I. N., 1985: Properties of suspended sediment over the HEBBLE area on the Nova Scotia Rise. *Mar. Geol.*, **66,** 169–188.

Maxey, M. R., and J. J. Riley, 1983: Equation of motion for a small rigid sphere in a nonuniform flow. *Phys. Fluids,* **26,** 883–889.

Mitchell, J. G., A. Okubo, J. A. Fuhrman and W. Cochlan, 1989: The contribution of phytoplankton to ocean density gradients. *Deep-Sea Res.*, **36,** 1277–1282.

Parsons, T. R., M. Takahashi and B. Hargrave, 1984: *Biological Oceanographic Processes,* 3rd ed. Pergamon Oxford, 330 pp.

Pearcy, W. G., and R. S. Mesecar, 1971: Scattering layers and vertical distribution of oceanic animals off Oregon. *Proc. Inter. Sym. on Biological Sound Scattering in the Ocean,* Report No. MC-005, G. B. Farquhar, Ed., Maury Center for Ocean Science, 381–394.

Phillips, O. M., 1980: *The Dynamics of the Upper Ocean.* Cambridge University Press, 336 pp.

Pieper, R. E., 1979: Euphausiid distribution and biomass determined acoustically at 102 kHz. *Deep-Sea Res.*, **26,** 687–702.

Pierce, J. W., 1976: Suspended sediment transport at the shelf break and over the outer margin. *Marine Sediment Transport and Environmental Management,* D. J. Stanley and D. J. P. Swift, Eds., Wiley, 437–458.

Pinkel, R., 1981: On the use of Doppler sonar for internal wave measurements. *Deep-Sea Res.*, **28,** 269–289.

——, 1983: Doppler sonar observations of internal waves: Wavefield structure. *J. Phys. Oceanogr.*, **13,** 804–815.

——, and J. A. Smith, 1987: Open ocean surface wave measurement using Doppler sonar. *J. Geophys. Res.*, **92,** 12 967–12 973.

Plueddemann, A. J., and R. Pinkel, 1989: Characterization of patterns of diel migration using a Doppler sonar. *Deep-Sea Res.*, **36,** 509–530.

Regier, L., 1982: Mesoscale current fields observed with a shipboard profiling acoustic current meter. *J. Phys. Oceanogr.*, **12,** 880–886.

Sheldon, R. W., A. Prakash and W. H. Sutcliffe, 1972: The size distribution of particles in the ocean. *Limnol. Oceanogr.*, **17,** 327–340.

Sherman, J. T., 1989: Observations of finescale vertical shear and strain in the upper ocean. Ph.D. thesis, University of California, San Diego, 145 pp.

Simon, M., and F. Azam, 1989: Protein content and protein synthesis rates of planktonic marine bacteria. *Mar. Ecol. Prog. Ser.*, **51,** 201–213.

Smith, J., R. Pinkel and R. A. Weller, 1987: Velocity structure in the mixed layer during MILDEX. *J. Phys. Oceanogr.*, **17,** 425–439.

Smith, J. A., 1989: Doppler sonar and surface waves: Range and resolution. *J. Atmos. Oceanic Technol.*, **6,** 680–696.

Stanton, T. K., R. D. M. Nash, R. L. Eastwood and R. W. Nero, 1987: A field examination of acoustical scattering from marine organisms at 70 kHz. *IEEE J. Oceanic Eng.*, **OE-12,** 339–348.

Tennekes, H., and J. L. Lumley, 1972: *A First Course in Turbulence.* The MIT Press, 300 pp.

Trump, C. L., B. S. Okawa and R. H. Hill, 1985: The characterization of a midocean front with a Doppler shear profiler and a thermistor chain. *J. Atmos. Oceanic Technol.*, **2,** 508–516.

Urick, R. J., 1983: *Principals of Underwater Sound.* McGraw Hill, 423 pp.

Veth, C., 1980: A laser Doppler velocimeter for small-scale turbulence studies in the sea. *Marine Science,* J. C. J. Nihoul, Ed., Elsevier, 303–317.

Wu, J., 1988: Bubbles in the near-surface ocean: A general description. *J. Geophys. Res.*, **93,** 587–590.